

MICROCOPY RESOLUTION TEST CHART
NATIONAL BUREAU OF STANDARDS-1963-A

12

AD-A173 087

DNA-TR-86-119

DEVELOPMENT OF A DRAG MEASUREMENT SYSTEM FOR THE CERF 6-FOOT SHOCK TUBE

**George H. Burghart
G B Laboratory, Inc.
201 W. Dyer Road, Unit B
Santa Ana, CA 92707-3426**

31 March 1986

Technical Report

CONTRACT No. DNA 001-84-C-0438

**Approved for public release;
distribution is unlimited.**

THIS WORK WAS SPONSORED BY THE DEFENSE NUCLEAR AGENCY
UNDER RDT&E RMSS CODE X342084469 Q93QMXAG00039 H2590D.

**Prepared for
Director
DEFENSE NUCLEAR AGENCY
Washington, DC 20305-1000**

**DTIC
ELECTE
OCT 15 1986
B**

DTIC FILE COPY

86 10 9 010

DISTRIBUTION LIST UPDATE

This mailer is provided to enable DNA to maintain current distribution lists for reports. We would appreciate your providing the requested information.

- Add the individual listed to your distribution list.
- Delete the cited organization/individual
- Change of address.

NAME: _____

ORGANIZATION: _____

OLD ADDRESS

CURRENT ADDRESS

_____	_____
_____	_____
_____	_____

TELEPHONE NUMBER: () _____

SUBJECT AREA(S) OF INTEREST:

_____	_____
_____	_____
_____	_____

DNA OR OTHER GOVERNMENT CONTRACT NUMBER: _____

CERTIFICATION OF NEED-TO-KNOW BY GOVERNMENT SPONSOR (if other than DNA):

SPONSORING ORGANIZATION: _____

CONTRACTING OFFICER OR REPRESENTATIVE: _____

SIGNATURE: _____

UNCLASSIFIED

SECURITY CLASSIFICATION OF THIS PAGE

AD-A173087

REPORT DOCUMENTATION PAGE				Form Approved OMB No. 0704-0188 Exp. Date: Jun 30, 1986	
1a. REPORT SECURITY CLASSIFICATION UNCLASSIFIED			1b. RESTRICTIVE MARKINGS		
2a. SECURITY CLASSIFICATION AUTHORITY N/A since Unclassified			3. DISTRIBUTION/AVAILABILITY OF REPORT Approved for public release; distribution is unlimited.		
2b. DECLASSIFICATION/DOWNGRADING SCHEDULE N/A since Unclassified					
4. PERFORMING ORGANIZATION REPORT NUMBER(S) GBL-86-036R			5. MONITORING ORGANIZATION REPORT NUMBER(S) DNA-TR-86-119		
6a. NAME OF PERFORMING ORGANIZATION G B Laboratory, Inc.		6b. OFFICE SYMBOL (if applicable)	7a. NAME OF MONITORING ORGANIZATION Director Defense Nuclear Agency		
6c. ADDRESS (City, State, and ZIP Code) 201 W. Dyer Road, Unit B Santa Ana, CA 92707-3426			7b. ADDRESS (City, State, and ZIP Code) Washington, DC 20305-1000		
8a. NAME OF FUNDING/SPONSORING ORGANIZATION		8b. OFFICE SYMBOL (if applicable)	9. PROCUREMENT INSTRUMENT IDENTIFICATION NUMBER DNA 001-84-C-0438		
8c. ADDRESS (City, State, and ZIP Code)			10. SOURCE OF FUNDING NUMBERS		
		PROGRAM ELEMENT NO 62715H	PROJECT NO Q93QMXA	TASK NO G	WORK UNIT ACCESSION NO. DH008769
11. TITLE (Include Security Classification) DEVELOPMENT OF A DRAG MEASUREMENT SYSTEM FOR THE CERF 6-FOOT SHOCK TUBE					
12. PERSONAL AUTHOR(S) Burghart, George H.					
13a. TYPE OF REPORT Technical		13b. TIME COVERED FROM 840928 TO 860301	14. DATE OF REPORT (Year, Month, Day) 860331		15. PAGE COUNT 42
16. SUPPLEMENTARY NOTATION This work was sponsored by the Defense Nuclear Agency under RDT&E RMSS Code X342084469 Q93QMXAG00039 H2590D.					
17. COSATI CODES			18. SUBJECT TERMS (Continue on reverse if necessary and identify by block number)		
FIELD	GROUP	SUB-GROUP			
13	13		Shock Tube		
20	11		Precursed Flow		
			Drag Measurement		
			Dynamic Pressure		
			Force Plates		
19. ABSTRACT (Continue on reverse if necessary and identify by block number)					
<p>An instrumentation system was developed that permitted the direct measurement of drag forces on flat plates in a precursed and/or dusty shock tube flow environment. The system was designed for very high frequency response to track the rapid changes in the shock tube flow. A fully self-contained data acquisition unit with solid state memory was also designed and built for this application. The system was fielded in the CERF 6-Foot Shock Tube at Kirtland Air Force Base, New Mexico.</p>					
20. DISTRIBUTION/AVAILABILITY OF ABSTRACT <input type="checkbox"/> UNCLASSIFIED/UNLIMITED <input checked="" type="checkbox"/> SAME AS RPT <input type="checkbox"/> DTIC USERS			21. ABSTRACT SECURITY CLASSIFICATION UNCLASSIFIED		
22a. NAME OF RESPONSIBLE INDIVIDUAL Betty L. Fox			22b. TELEPHONE (Include Area Code) (202) 325-7042		22c. OFFICE SYMBOL DNA/STTI

DD FORM 1473, 84 MAR

83 APR edition may be used until exhausted
All other editions are obsolete

SECURITY CLASSIFICATION OF THIS PAGE

UNCLASSIFIED

**CONVERSION FACTORS FOR U.S. CUSTOMARY
TO METRIC UNITS OF MEASUREMENT**

To Convert From	To	Multiply By
degree (angle)	radian (rad)	1.745 329 X E -2
foot	meter (m)	3.048 000 X E -1
inch	meter (m)	2.540 000 X E -2
pound-force/inch ² (psi)	kilo pascal (kPa)	6.894 757



Accession	
NTIS	✓
DTIC	
Ver	
Jan	
By	
Date	
App	
Dist	
A-1	

TABLE OF CONTENTS

<u>Section</u>		<u>Page</u>
	CONVERSION TABLE.....	iii
	LIST OF ILLUSTRATIONS.....	v
1	INTRODUCTION.....	1
2	OBJECTIVES.....	2
3	DESCRIPTION OF THE EXPERIMENTAL APPROACH.....	3
	Background.....	3
	Design of the Drag Measurement System.....	5
	Design of the Drag Bodies.....	8
	Design of the Data Acquisition Unit.....	11
	System Design.....	11
	Hardware Description.....	13
	Data Acquisition Unit.....	16
4	CALIBRATION OF THE DRAG MEASUREMENT SYSTEM.....	17
5	EXPERIMENTAL RESULTS.....	19
6	LIST OF REFERENCES.....	29

LIST OF ILLUSTRATIONS

<u>Figures</u>		<u>Page</u>
1	DRAG COEFFICIENTS FOR BLUNT CYLINDERS, END ON.....	6
2	SCHEMATIC OF FORCE BODY.....	9
3	FORCE BODY PREAMP CIRCUIT.....	10
4	RAKE INSTALLATION IN 6-FOOT SHOCK TUBE.....	12
5	FORCE BODY/DIGITIZER CALIBRATION RESULTS.....	18
6	EXPERIMENT LOCATION IN 6-FOOT SHOCK TUBE.....	20
7	MEASURED DRAG FORCE, RUN 7, CLEAR AIR.....	22
8	MEASURED DRAG FORCE, RUN 8, CLEAR AIR.....	24
9	MEASURED DRAG FORCE, RUN 6, 11.5 Ft. HELIUM PRECURSER.	26

SECTION 1

INTRODUCTION

Vehicles and structures exposed to the air blast produced by nuclear weapons are subject to the two types of loading. The loads produced by the reflection of shock waves are termed diffraction loads and are rather readily measured and calculated. The forces produced by the interaction of the flow field behind the shock with the structure are termed drag loads and their determination is more difficult and requires information on more environmental parameters. In the thermally precursed flow, the diffraction loads and static overpressures are reduced and drag loading is greatly enhanced. Scaling from subscale simulators to the full scale environment requires a knowledge of the dynamic pressure of the simulator flow.

The determination of the dynamic pressure in clean fluid mechanical flow is achieved by measurements of side-on and total pressure and measurement or a-priori knowledge of certain fluid properties. In the presence of thermal gradients or gas mixtures and in particular for solid/gas mixed phase flow, the determination of dynamic pressure becomes quite difficult. This problem is further complicated by the likely existence of slip between the solid and gaseous phases in the simulator.

The approach for the determination of dynamic pressure in the simulator environment, followed here, uses the direct measurement of forces on drag bodies having well defined, and nearly constant, drag coefficients over a wide range of the Reynolds and March numbers. The determination of the effective dynamic pressure from force measurements is then reduced to simple arithmetic and the contributions of dust and thermal precursing to the effective dynamic pressures are included. When the dynamic pressure due to the gaseous phase only is known from other measurements, the dust concentration can be derived from the force data.

SECTION 2
OBJECTIVES

The objective of this program was to develop a drag measurement system compatible with the precursed and dusty environment of the NMERI 6-foot shock tube and to design and build a self-contained data acquisition and storage system.

SECTION 3

DESCRIPTION OF THE EXPERIMENTAL APPROACH

3.1 BACKGROUND.

The application of fluid mechanical test data to predict responses of geometrically similar objects in environments different from the test environment involves a technique known as "model testing." This technique is needed when test facilities cannot accommodate full scale prototypes or test conditions cannot be made to match the environmental parameters of the intended applications. The principles of model testing are based essentially on dimensional analysis which has been formalized into what is known as the π -theorem. (Ref. 1).

From such dimensional analyses result the familiar dimensionless pressure and force coefficients,

$$C_p = \frac{P}{\frac{1}{2} \rho V^2} \quad (1) \quad \text{and} \quad C_F = \frac{\text{Force}}{\frac{1}{2} \rho V^2 A} \quad (2)$$

which in general are also functions of the familiar dimensionless lumped parameters of

$$\text{Reynolds number } R = \frac{\rho V L}{\mu} \quad \text{and} \quad \text{Mach number } M = \frac{V}{a}$$

The effects of viscosity (R) and compressibility (M) are known from experience and insight into the physics of the problem. The force coefficients are known to be constant within certain ranges of these parameters.

It must be pointed out that the statement above concerning the effect of Reynolds number may not apply to objects being tested within the boundary layer of the flow. A different set of scaling rules that govern flow separation must be applied there. It may be said in general that the ratio of obstacle height to boundary layer momentum thickness should be preserved for proper scaling, for objects on the order of one boundary layer thickness high.

For compressible ideal gas flows the dynamic pressure (q) is calculated from the equation

$$q = \frac{1}{2} \rho V^2 = \frac{1}{2} \gamma P_s M^2 \quad (3)$$

and the end-on pressure becomes $P_{t,2}$ which is the stagnation pressure behind the normal shock. The Mach number M is given by the Rayleigh pitot formula which involves the measured pressures and the ratio (γ) of the specific heats of the gas.

In the case of dusty flow the determination of effective dynamic pressure by pressure measurement techniques is virtually impossible, except for the very special case, analyzed by Marble, (Reference 2), where solid and gas phases are in complete equilibrium so that the combined phases respond as a perfect gas. For that special case it becomes possible, in principle, to treat the effect of dust as a modification of density, specific heat, and molecular weight of the gaseous medium.

For the drag measurement technique to determine the effective dynamic pressure, an a-priori knowledge of the dust concentration is not required, nor is the precise state of equilibrium a prerequisite. Although the effective dynamic pressure determined by this method may not be readily interpreted as the product of mean density and velocity squared, it will be the proper driving function that produces loads on structures.

For this application it is reasonable to allow impacts of solid particles on the drag bodies. The frontal area is normal to the incident dust, and the front surface can be designed to prevent particle rebound. The contribution of solid dust particle impacts to the measured drag force is then equal to the incident dust momentum.

The specific approach described in the following sections fielded arrays of flat circular disks, mounted normal to the incident flow of the 6 foot NMERI shock tube with and without helium precursing.

3.2 DESIGN OF THE DRAG MEASUREMENT SYSTEM.

The design requirements of the drag measurement system are dictated by the test environment. The primary difficulty in this design approach stems from the rapidly changing environment of the shock simulator flow. A high frequency response is therefore important, which dictates low mass and high stiffness. Data interpretation is simplified if the system can be designed for minimum variation in force coefficients. Dependence on Mach number is not readily eliminated, however, Reynolds number dependence is virtually eliminated if the measurement is limited to forebody drag, i.e. base drag is eliminated. Further, if the force disk is short in the streamwise direction, friction drag may also be neglected. A thin, flat, circular disk, supported over its entire base region was therefore selected for this application. The drag coefficient (forebody only) for this configuration is independent of Reynolds number from 10^3 to 10^7 and varies with Mach number as shown in Figure 1 (Reference 3)

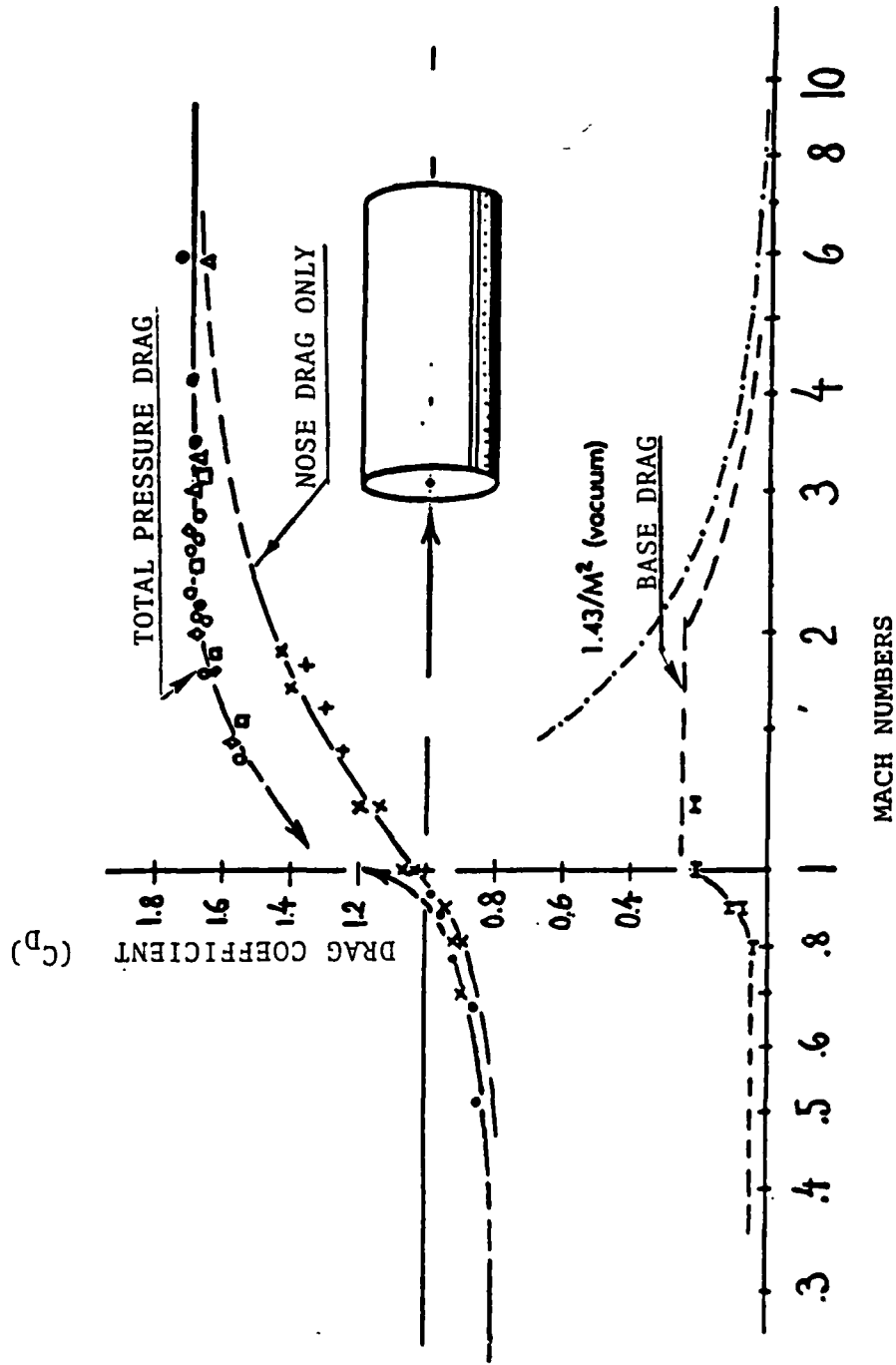


Figure 1. Drag coefficients for blunt cylinders, end on.

The upper limit of frequency to which a force measurement system can accurately respond is the natural mechanical frequency of the measurement system. To achieve high frequency response a force measurement system must therefore be both light and stiff along the sensitive axis.

Only two basic sensing elements are in widespread use in high frequency systems; the strain gage, and the piezoelectric element. The mechanical compliance is governed only by the constraints required to produce a measurable strain in a short section of the structure. Complications caused by the use of strain gages for force measurements are the need for an excitation power and for larger differential signal amplification. One of the biggest advantages of a strain gage force measuring system is that it can measure steady state forces, which greatly simplifies precision calibration by static loading.

The piezoelectric element consists of a thin wafer of a crystal or polarized ceramic. During compression an electrical charge is generated on the face of the element. The magnitude of the charge is proportional to the applied compressive force. Because of charge leakage, piezoelectric elements are unsuited for steady-state force measurements and unfortunately, also static calibration. On the other hand the extreme stiffness and high sensitivity of the piezoelectric element make their use attractive for the transient force measurements of this application.

Piezoelectric materials are also known to be sensitive to temperature changes. Fortunately, for the short duration of the application here, and the low expected heat fluxes, it is not particularly difficult to provide thermal protection.

3.3 DESIGN OF THE DRAG BODIES.

A very simple, but particularly high frequency system was configured for the initial entry into the 6-foot shock tube. The force body was basically one surface of the piezoelectric wafer. This surface was protected only by a 0.020 inch thick layer of soft rubber, attached to the wafer with an ultrasonic coupling grease. The wafer was then attached to a 1/4 inch thick steel plate using a conducting epoxy. The plate was mounted on a 1/2 inch thick sting which flaired out to a 1 inch cylinder.

After exposure to the shock tube environment and some quasi-steady calibrations it was discovered that the back-up structure was not sufficiently stiff. Bending of the assembly produced large signals that were not proportional to the applied load. It was clear that a full diameter sting would be required. The system was therefore redesigned accordingly (Figure 2). A number of other minor changes were also incorporated. The configuration fielded during the second shock tube entry consisted of a full diameter sting, to support the ceramic wafer. The front face of the transducer was then covered over with duct tape to protect it from particle impacts and isolate it from any electrical charge that might be generated by small particle impacts.

The use of a charge device requires short and/or highly protected lead wires. For this purpose the line lengths were limited to less than 6 inches and terminated in an amplifier. A two-stage preamplifier was designed and built for this purpose as shown in Figure 3. The first stage had an adjustable gain of nominally 1 to 11 and the second stage had a fixed gain of 5.7. Thus it was possible to set a 0 to 5 volt output for the expected force range of each transducer.

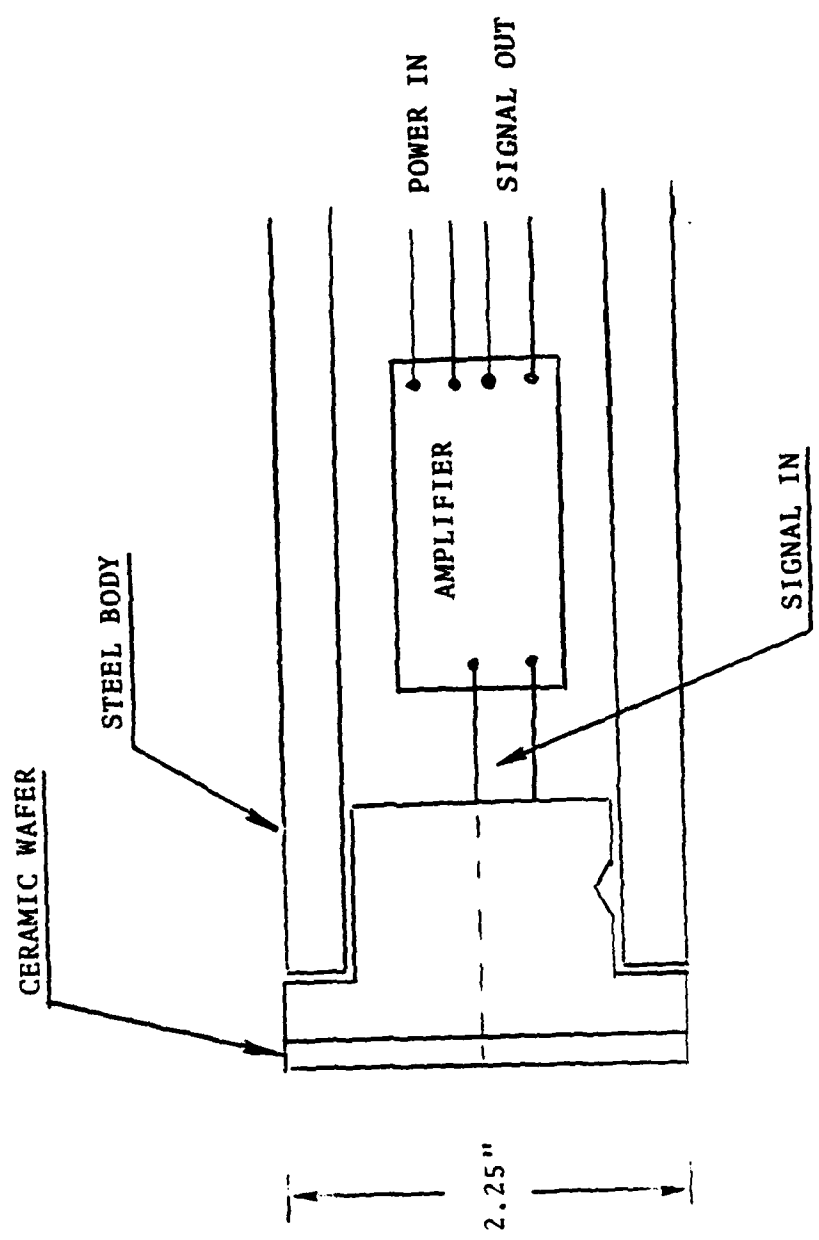


Figure 2. Schematic of force body.

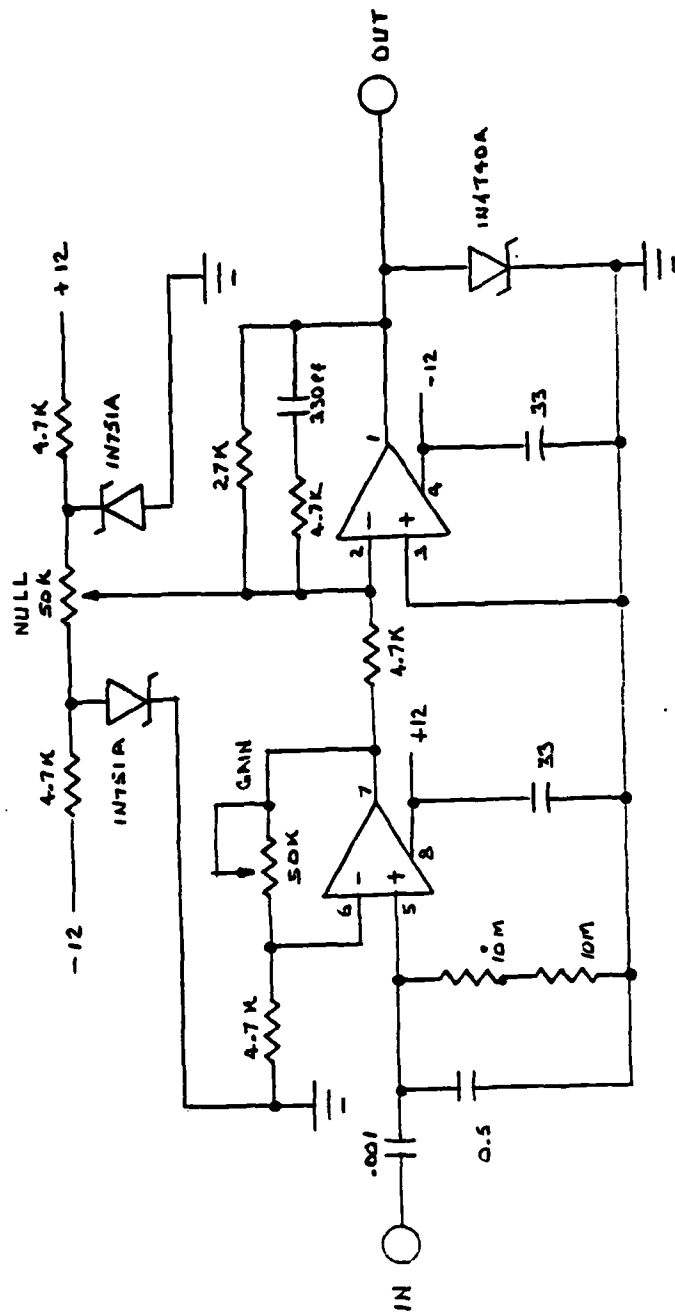


Figure 3. Force body preamp circuit.

The force bodies were mounted in-line on a strut that spanned the shock tube. The actual heights above the ground are shown in Figure 4, as installed in the shock tube.

To demonstrate the feasibility of recording such data on site, in solid state memory, a completely self-contained data acquisition and recording system was designed and built. All electrical power was internal and furnished by D C batteries.

3.4 DESIGN OF THE DATA ACQUISITION UNIT.

The data acquisition unit (DAU) was a self-contained, low power CMOS system which acquired, digitized, and stored analog data from transducers during testing. The DAU chassis contained 5 channels of analog input and provided its own power source via an internal or external battery. After data storage has taken place the units are transported to a computer for data retrieval. The solid state memory had its own internal data retention battery with a life of 10 years.

3.4.1 System Design.

The DAU consisted of the chassis, the battery, and the card cage. The card cage contained the acquisition card, the memory control card, the memory card(s), and the power supply. A modular design approach was selected for the data acquisition unit. Customization of the units to suite specific requirements was therefore readily possible. The chassis could be designed to be compatible with adverse environments. For the shock tube application the chassis was made dust and to some extent water tight so that it could be fielded outdoors at the 6 foot shock tube site. The battery to power the DAU could be internal or external and battery size could be selected

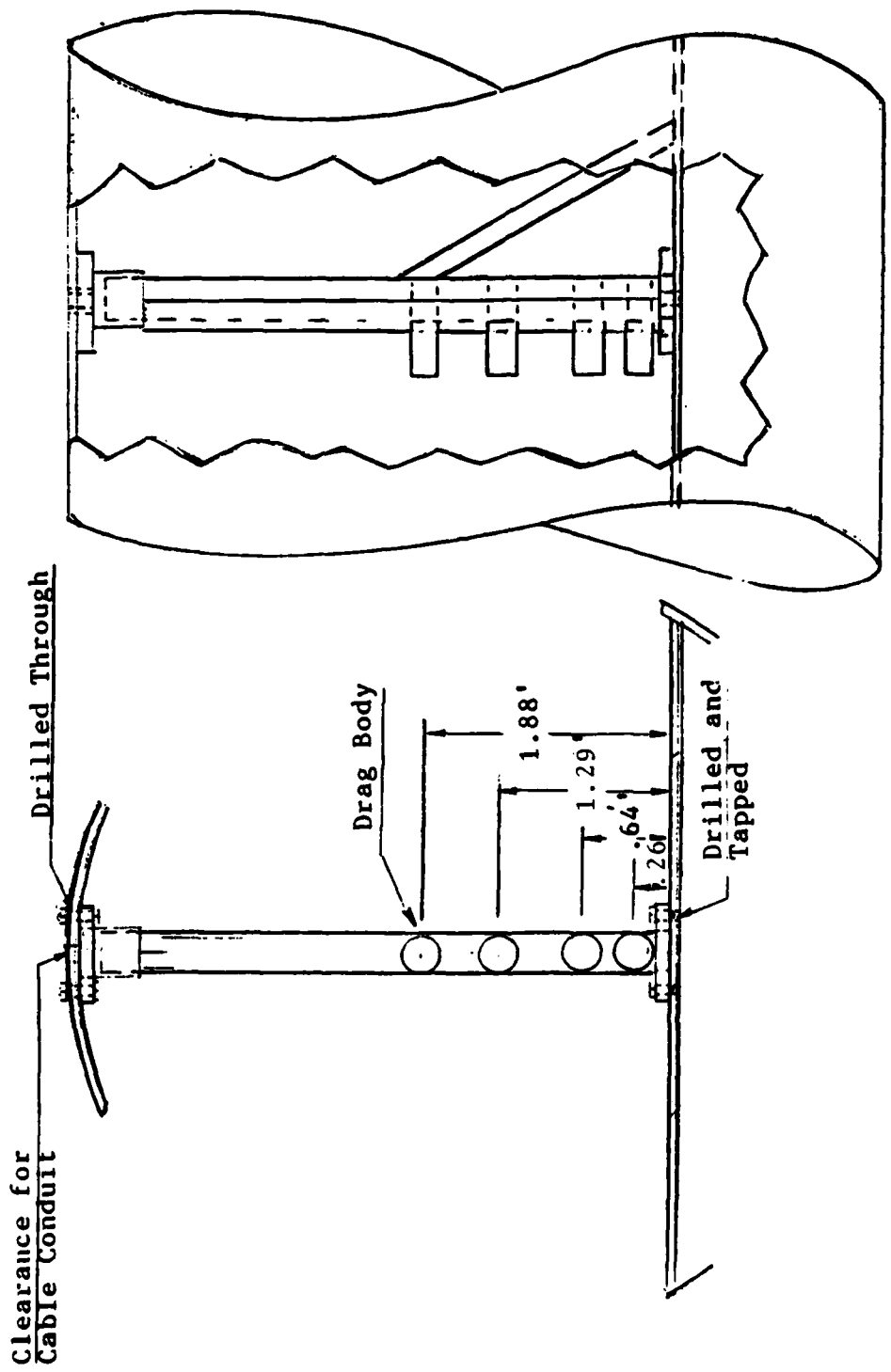


Figure 4. Rake installation in 6-foot shock tube

to suit the desired life expectancy. For the shock tube application a 12 volt Panasonic re-chargable battery was used, housed within the chassis. The number of channels to be recorded could also be varied between 1 and eight and the size of the memory could readily be expanded to one Mega-Byte. Four channels of data were recorded here and the memory was limited to 64K total.

The data acquired by the data acquisition card was written into the memory of the DAU under the control of the memory controller. The data was later read from the memory by a computer. When triggered the memory controller commands all of the acquisition cards to convert the analog input into digital format at the same time. Thus all of the channels within a DAU were time synchronized. Once the digital values were available, the memory controller caused each acquisition card to write the converted values into consecutive memory locations. Then the memory controller waited until the next samples were to be taken and then repeated the process. This was done until all of the memory had been filled with data.

To retrieve the data, a computer was programmed to interface with the DAU via a parallel port. The data was transferred as parallel bytes with each channel in successive locations.

3.4.2 Hardware Description.

Chassis

The chassis design was very much application dependent. It contained the battery and the card cage safely in the intended environment. It had a terminal strip, external to the container to facilitate connection of external inputs

Battery

The battery required an output of 12 Volts since line losses were minimal. The capacity requirement was variable and depended on the number of channels to be recorded and the size of the memory. Since it was only necessary to operate the data acquisition unit for a few minutes per run, the capacity required of the battery was minimal.

Card Cage

The card cage implemented the CMOS STD bus. The bus used was an industry standard for low power data acquisition systems. Thus the DAU could be used for many different applications with the purchase of off-the-shelf cards from many different manufacturers. The card cage contained all of the electronics for the DAU.

Power Supply

The power supply accepted an input in the range from 9V to 18V DC. The output is +5V and +/-15V. The output went to the CMOS STD Bus and to a connector on the top of the card for powering the transducer preamps. The input to the power supply was fuse protected.

Acquisition Card

The acquisition card accepted the output of the transducer/preamp in the form of a voltage between 0 and +5V. This signal was subjected to a low pass filter which limited the bandwidth to eliminate the aliasing caused by the digitization. The filtered signal was input to a sample and hold to provide a stable input to the analog to digital converter. The converter converted the signal to a 8-bit digital value. This digital value was then temporarily stored in a latch prior to being written into memory at the appropriate time.

Memory Control Card.

The memory control card controls the acquisition of data, the storing of this data, and the retrieval of the stored data. When triggered, the acquisition of data continued until the entire memory had been filled. The sequence of events was as follows: The acquisition cards were simultaneously commanded to sample the incoming signal and then convert this held signal into a digital value. Once the digital value was available, the memory controller commanded each acquisition card individually to place the data on the CMOS STD Bus. Then the memory controller created the signal to write this data into memory. This continued until all the channels had been read. To retrieve the data, the memory controller read successive memory locations and transferred this data to the parallel output.

Memory Card.

The memory card was a CMOS STD Bus card with a memory capacity of 64K Bytes. Up to sixteen memory cards could be used in a single system allowing a maximum of 1 Mega byte of data storage. The memory chips used were very low power devices that had lithium batteries built into them. These batteries allowed the acquired data to be stored for up to 10 years regardless of the condition of the system battery.

The capabilities and specifications of a data acquisition unit are summarized on the next page.

DATA ACQUISITION UNIT

Number of Channels: 5

Sample Rate: 25 KHz, 50 KHz, 100 KHz
(Time synchronized)

Memory: 13,000 words/channel, 64K total

Resolution: 8 bits

Record Time: 520 mS, 260 mS, 130 mS

Data Retention Time: 10 years
(Batteries inside RAM chips)

Power: 9 - 18 VDC (nominal 12 V battery)

Operating Current: 200 mA
(Only when armed)

Data Transfer: Parallel format
(Compatible with many computers)

Mass Storage: Floppy Disks

Hardcopy: Plot on printer
Numerical data on printer

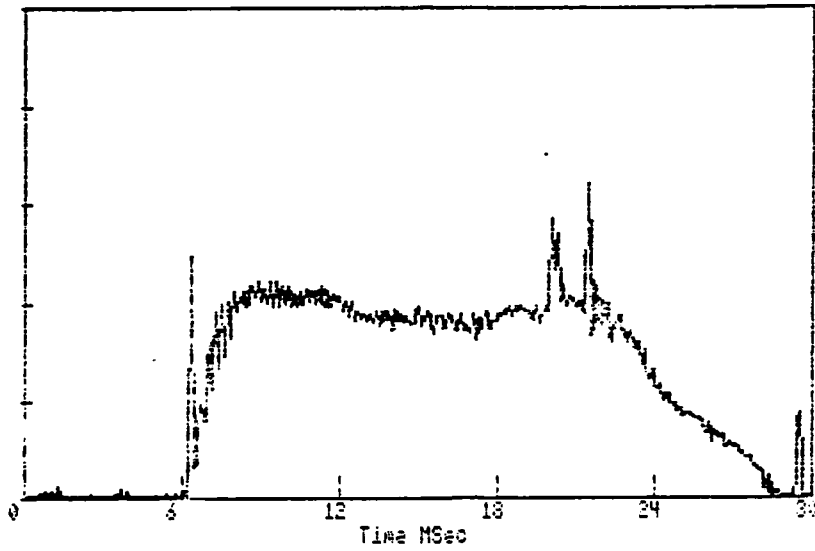
SECTION 4

CALIBRATION OF THE DRAG MEASUREMENT SYSTEM

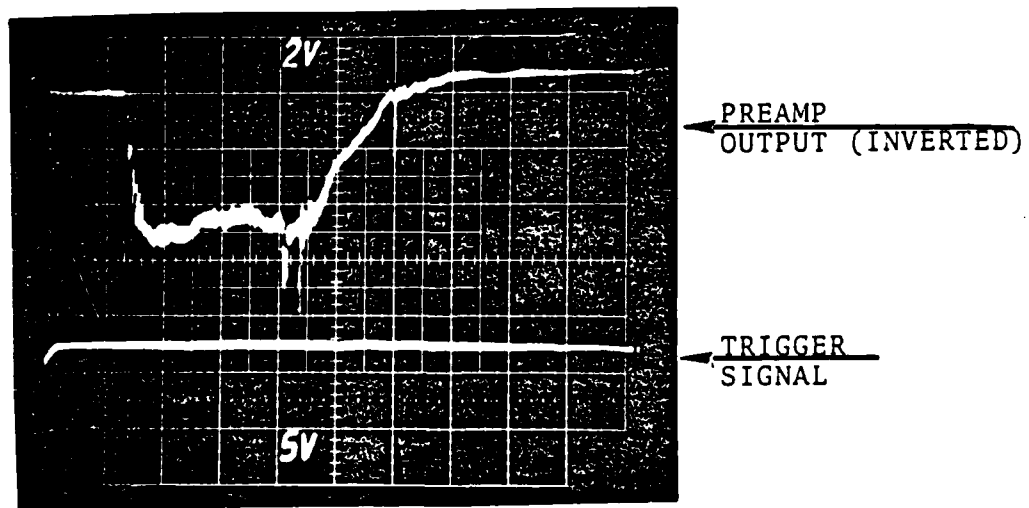
The successful implementation of any measuring system depends largely on its calibration. The objective of such a calibration effort must be to test the response of the system to all of the important test parameters expected in the field test environment. When feasible, the calibration should cover the entire range of expected field test parameters. Unfortunately it is usually not possible to simulate the entire expected test environment in the laboratory.

The calibration in the G B Laboratory shock tube was limited to low pressure runs, a facility limitation at GBL. These runs did however meet the primary calibration objective, namely the demonstration of the frequency response, the performance of the preamp, and the proper functioning of the data acquisition system. A typical response of the force measuring system is shown in Figure 5. The comparison of the oscilloscope trace of the analog output of the preamp and the plot of the digitized data retrieved from memory shows excellent agreement. The scope trace is inverted. Also it must be noted that the digital system cannot reproduce negative values.

A quasi-steady, dead load calibration was also performed in the laboratory. A load was applied quickly in a mechanical press and measured by a load cell. The transducer outputs were found to be consistent with the calculated performance.



a. Plot of digitized data.



Time, 5 msec per Division

b. Analog signal from force body.

Figure 5. Force body digitizer calibration results.

SECTION 5

EXPERIMENTAL RESULTS

The facility was first entered on 23 April 1985. The model installation was made at the 133 foot station as indicated in the facility schematic of Figure 6. Five mostly unsuccessful runs were performed on a piggy-back basis with other experiments. This series of runs produced no usable force data but provided important information that was used in the redesign of the drag bodies. Excessive bending of the back-up structure that held the piezoelectric wafers was the primary problem. The much stiffer structure of Figure 2 was therefore implemented. Also greater rigidity of the mounting strut seemed desirable which was accomplished by providing a structural brace.

The facility was then revisited on 7 May 1985 and a series of three successful runs was completed. Data was recorded for four force bodies for each run at heights above the floor of 0.26, 0.64, 1.29 and 1.88 feet respectively. The data presented in the following figures is the actual measured force experienced by the four square inch force plates.

To compare the present data to other measurements in that facility we have calculated the force to be expected based on the drag coefficients of Figure 1 and the dynamic pressure in the facility. The Mach number and the dynamic pressure for the facility were determined from reported side-on (static) and end-on (total) pressure measurements. Unfortunately only very limited pressure data was recorded by NMERI during these runs. It was therefore necessary to resort to data recorded for similarly configured runs performed by NMERI during earlier efforts.

No data could be found for the 133 foot station. The closest measurement station for similarly configured runs was at 126.8 feet. Run number HSTS6-77 was selected for the clean configuration and Run number HSTS6-75 was used for comparison

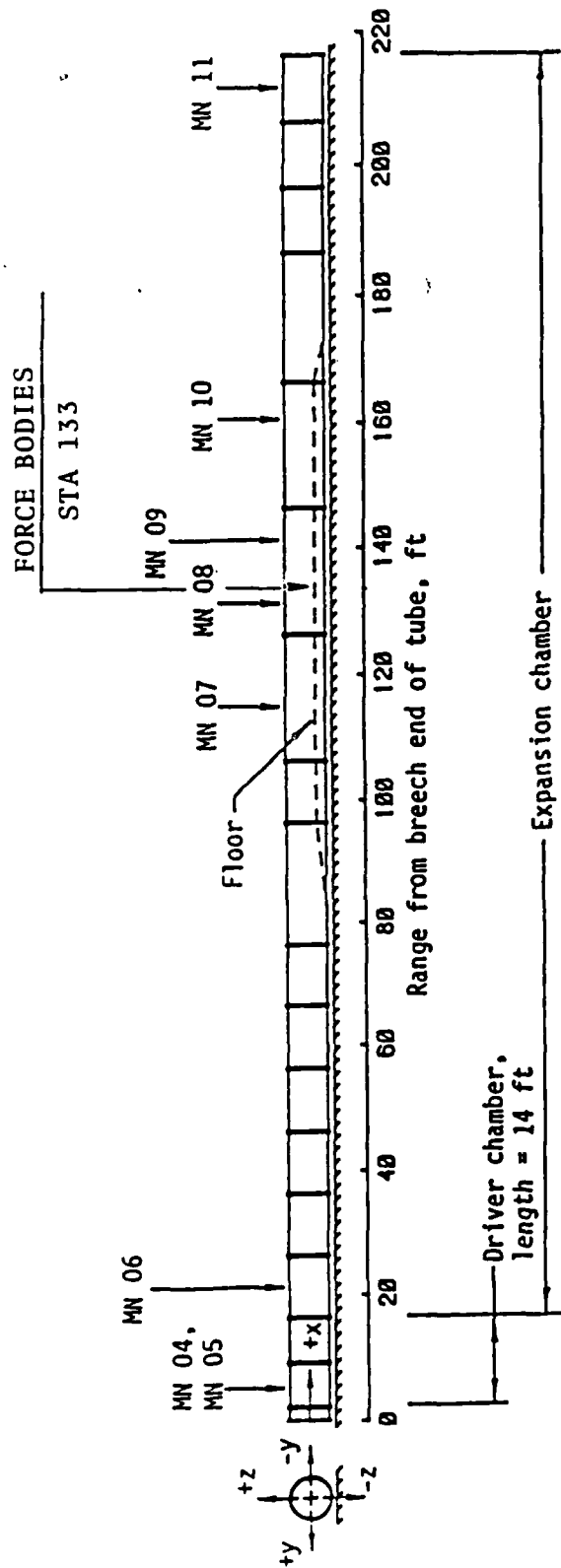


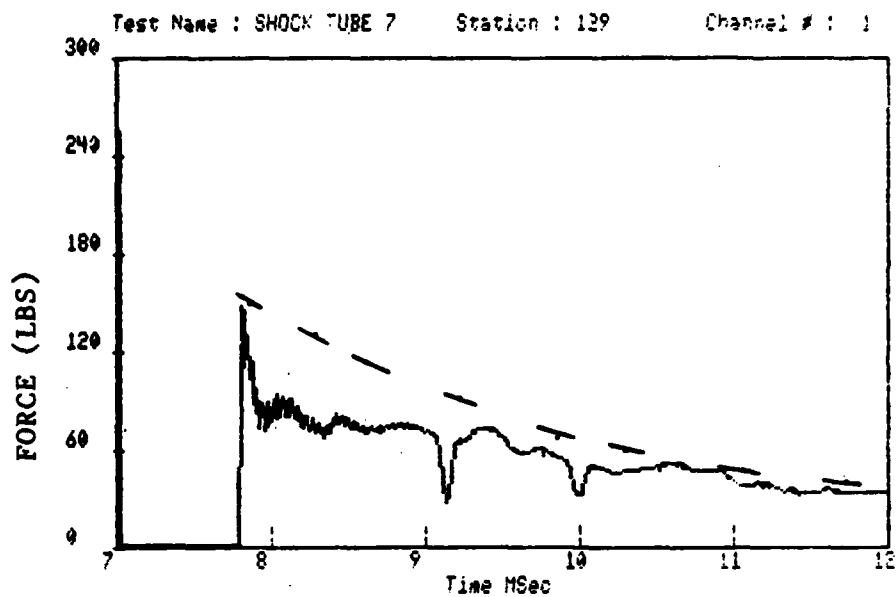
Figure 6. Experiment location in 6-foot shock tube.

with the thermally precursed data of this experiment which also had an 11.5 long, 5 inch thick Helium layer immediately upstream of the measurement station.

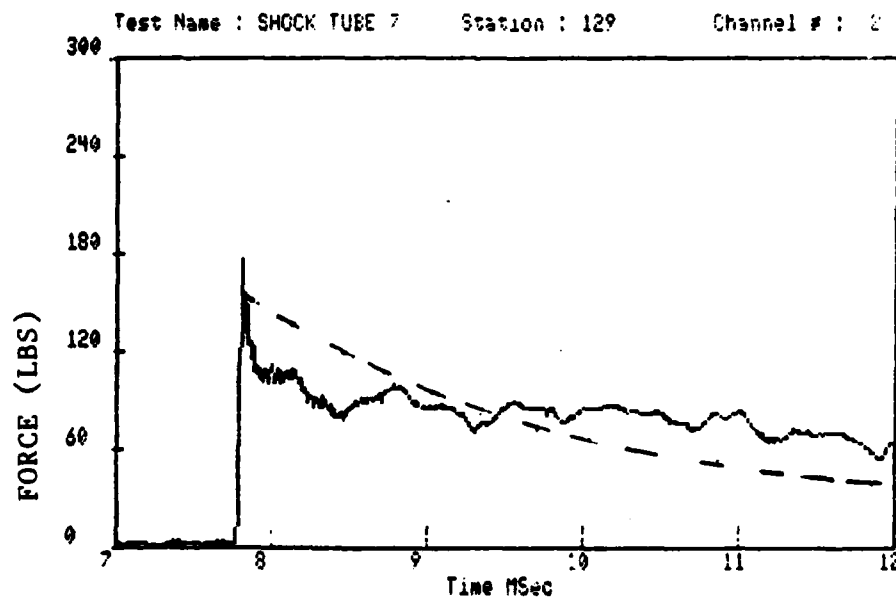
The forces calculated for the clear air shot are superimposed on the the measured force data from the present runs as seen in Figures 7 and 8 for runs # 7 and 8 respectively. The agreement is seen to be reasonably good between measurement and prediction. The amplitudes are somewhat different but the shape of the profiles is well predicted. Particularly good run-to-run repeatability is seen when the data from run 7 is compared to run 8. This excellent repeatability suggests that the force measurement system was working properly.

The force data recorded for the Helium precursed run (number 6) is shown in Figure 9. Again insufficient pressure data was recorded to permit comparison of the force data to predictions. Unfortunately, the data of run HSTA6-75 was also judged unusable. First it was noted that except for a small difference in arrival time, the static pressure profile overlaid the un-precursed pressure profile exactly. Also the measurements at greater ground heights agreed exactly with the data of Run HSTS6-77. Only the lowest probe (at $\frac{1}{2}$ inch ground height) yielded a different response. The shape of the profile is however identical to those at greater ground heights and only the amplitude is slightly lower. This more nearly suggests a boundary layer effect rather than thermal precursing. Data comparison was therefore not reasonable.

The shapes of the measured drag profiles are judged to be representative of precursed flow. All gages, particularly in close ground proximity, showed a slow rise in drag initially, followed by a very sharp increase, unfortunately into gage saturation for low ground heights. The gages recovered however and revealed a second peak in drag, typical of precursed flows.

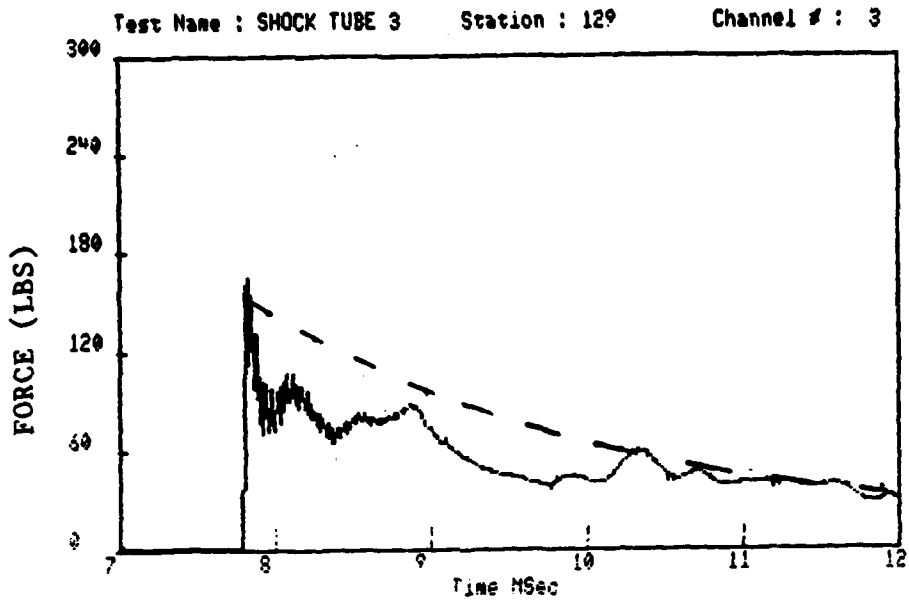


a. Height: 1.88 feet.

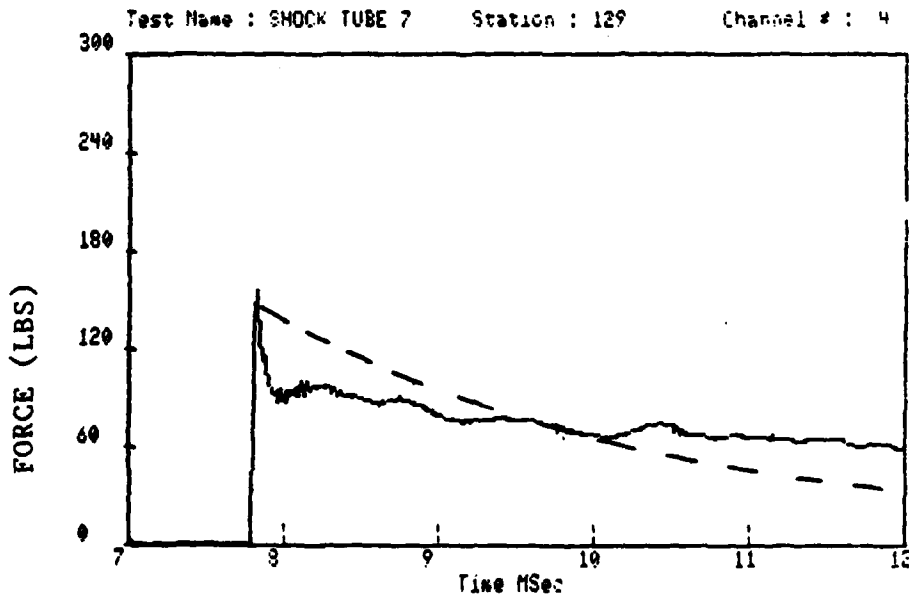


b. Height: 1.29 feet.

Figure 7. Measured drag force, run 7, clear air.

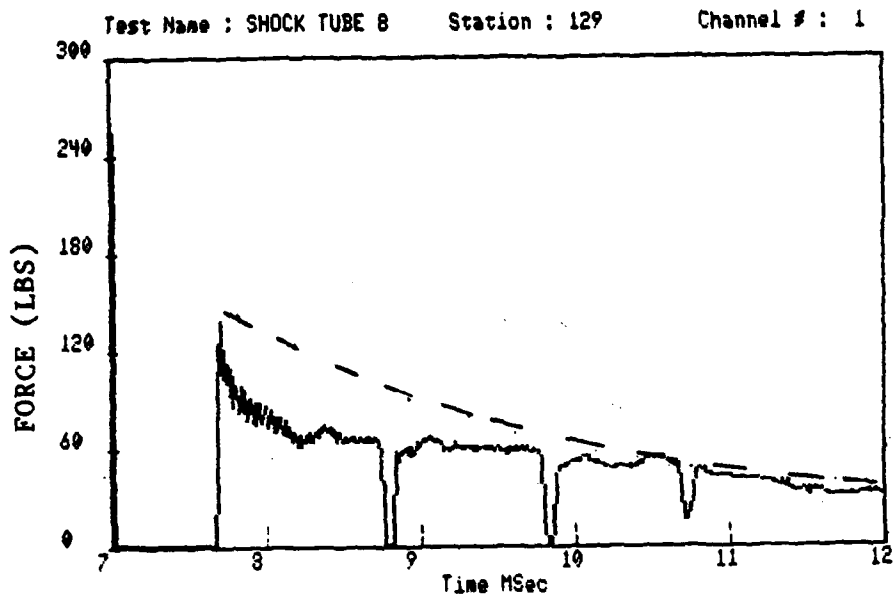


c. Height: 0.64 feet.

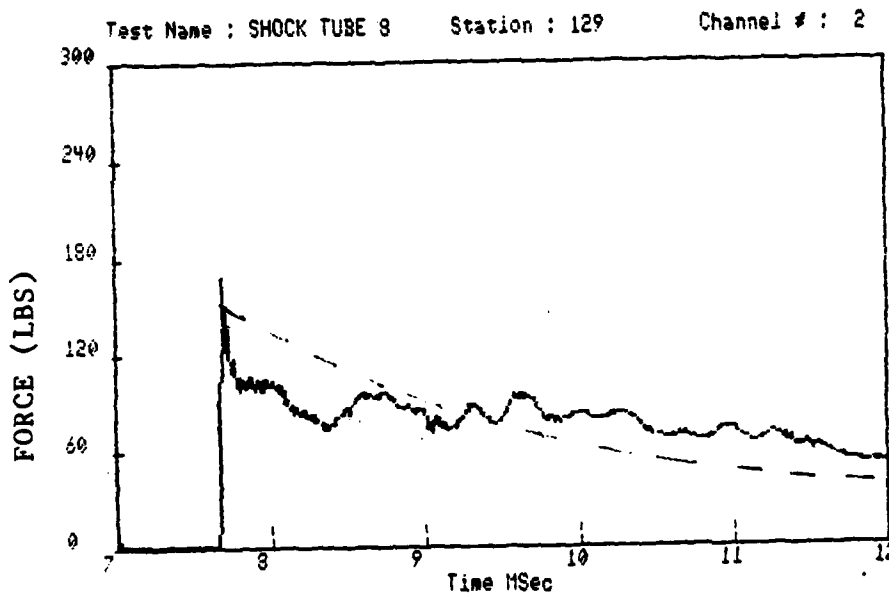


d. Height: 0.26 feet.

Figure 7. Measured drag force, run 7. (concluded)

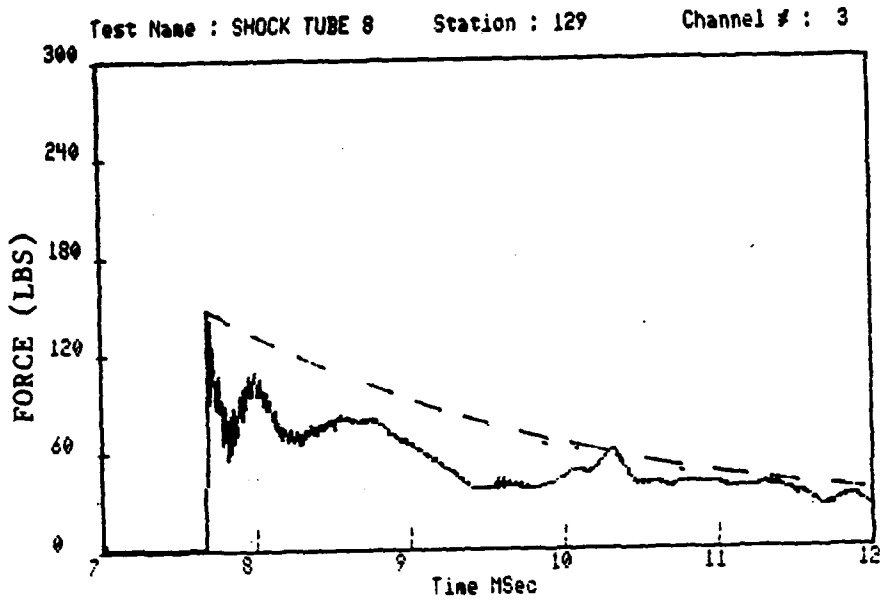


a. Height: 1.88 feet.

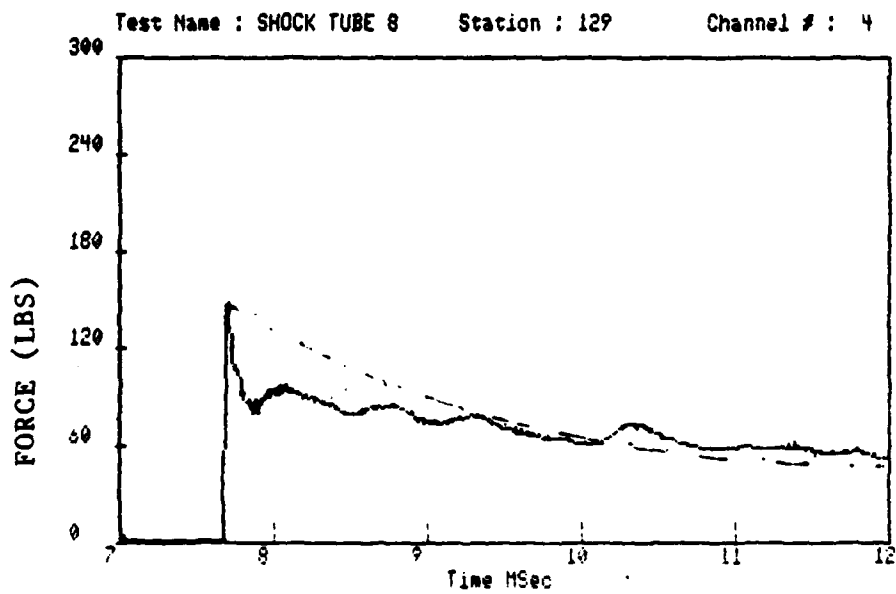


b. Height: 1.29 feet.

Figure 8. Measured drag force, run 8, clear air.

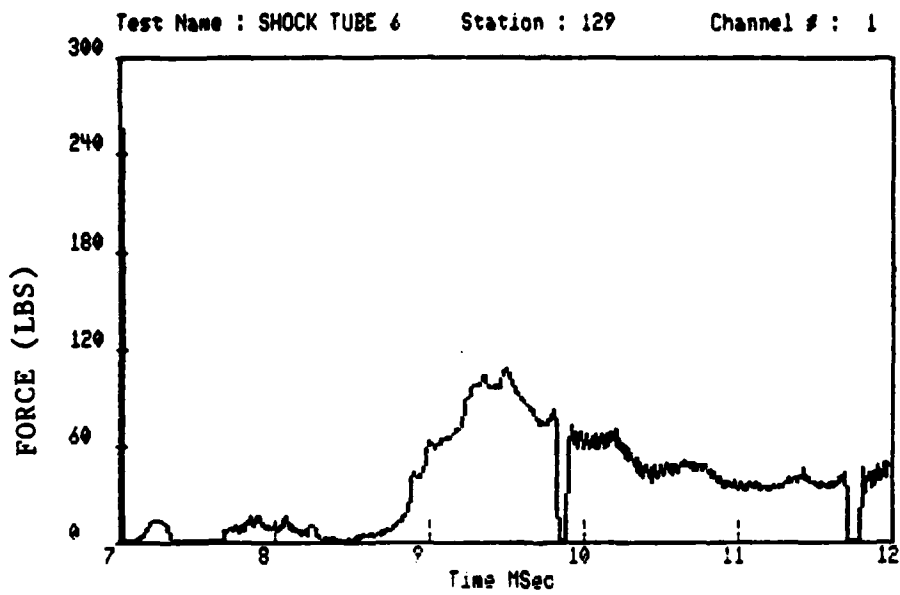


c. Height: 0.64 feet.

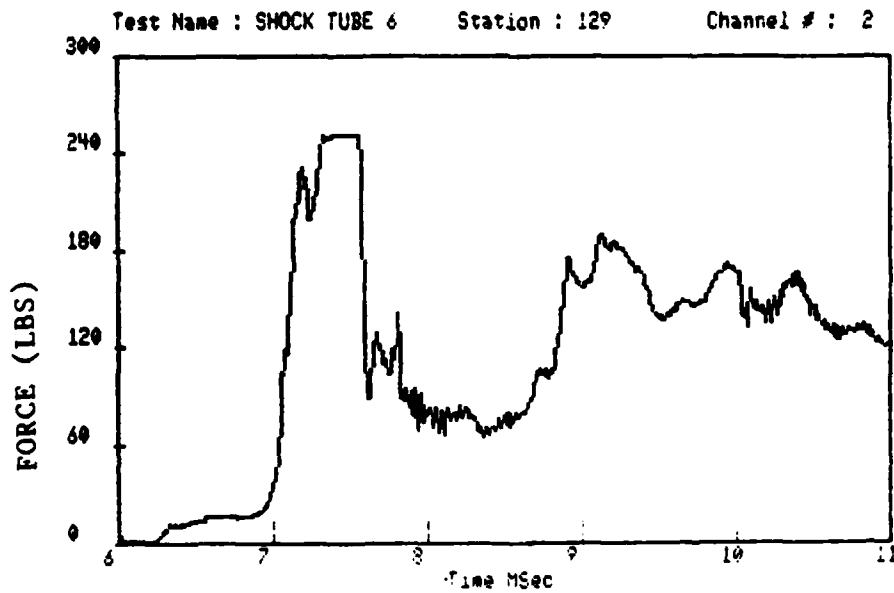


d. Height: 0.26 feet.

Figure 8. Measured drag, run 8. (concluded)

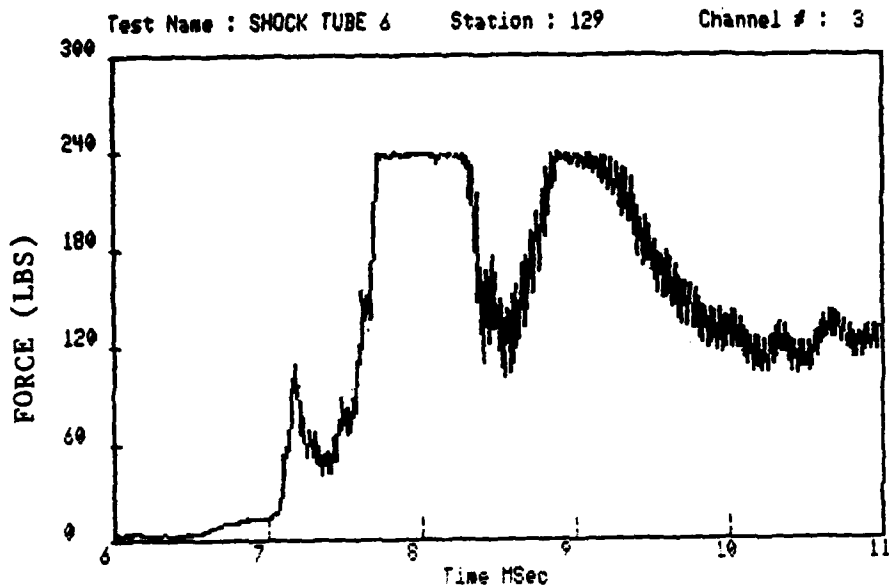


a. Height: 1.88 feet.

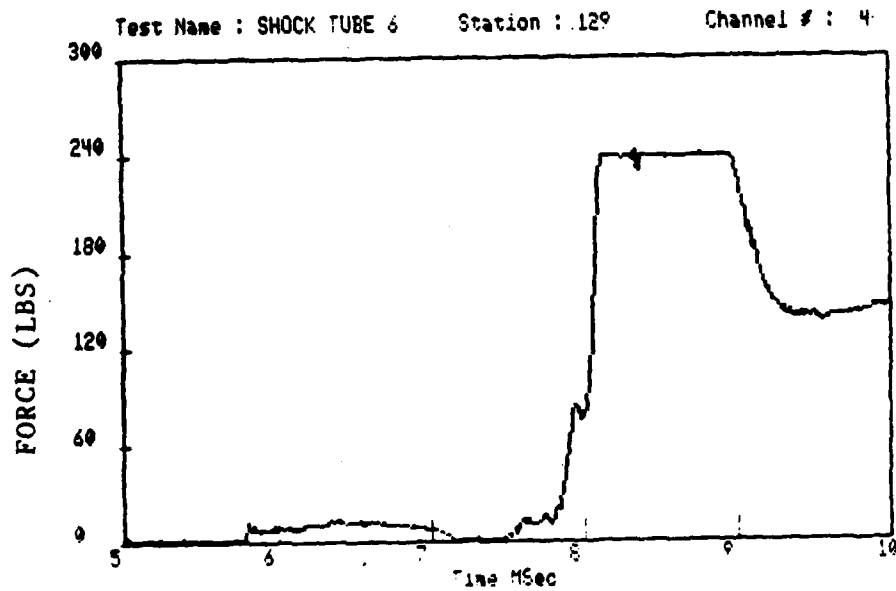


b. Height: 1.20 feet.

Figure 9. Measured drag force, run 6,
11.5 ft. helium precursor.



c. Height: 0.64 feet.



d. Height: 0.26 feet.

Figure 9. Measured drag force, run 6. (concluded)

Shock tube scheduling constraints made it necessary at that time to vacate the facility. Our efforts focused on the fielding of drag measurement systems at the Minor Scale event. Similarly configured drag body systems were fielded on the dusty, precursed region of the Minor Scale event at 50 and 30 psi static overpressure locations. The systems fielded functioned properly and clearly demonstrated that the drag measurement system had been successfully implemented (Reference 4). In light of the success at the Minor Scale and significant scheduling problems at the shock tube, it was decided that a revisit to the 6 foot shock tube was not necessary.

LIST OF REFERENCES

1. Buckingham, E. "Notes on the Method of Dimensions,"
Phil. Mag. 42, 696-719 (1921).
2. Hoerner, S. F. Fluid-Dynamic Drag, 1965.
3. Marble, F.E. "Dynamics of Dusty Gases", An. Rev. of
Fld. Mech. Vol. 2, 397-446 (1970).
4. Burghart, G.H. "Force and Dust Measurements"
Minor Scale Results Symposium,
28 February 1986.

11/11/11

DISTRIBUTION LIST

DEPARTMENT OF DEFENSE

AIR FORCE SOUTH

ATTN: U S DOCUMENTS OFFICER

ASST TO THE SECY OF DEFENSE ATOMIC ENERGY

ATTN: EXECUTIVE ASSISTANT

DEFENSE INTELLIGENCE AGENCY

ATTN: DT-2

ATTN: RTS

ATTN: RTS-2B

DEFENSE NUCLEAR AGENCY

ATTN: SPAS

ATTN: STSP

4 CYS ATTN: STTI-CA

DEFENSE TECHNICAL INFORMATION CENTER

12 CYS ATTN: DD

FIELD COMMAND DNA DET 2

LAWRENCE LIVERMORE NATIONAL LAB

ATTN: FC-1

FIELD COMMAND DEFENSE NUCLEAR AGENCY

ATTN: FCPR

ATTN: FCT COL J MITCHELL

ATTN: FCTT W SUMMA

ATTN: FCTXE

JOINT CHIEFS OF STAFF

ATTN: J-5 NUC & CHEM DIV

JOINT STRAT TGT PLANNING STAFF

ATTN: JLK (ATTN: DNA REP)

ATTN: JLKS

ATTN: JPPFM

ATTN: JPTP

UNDER SECY OF DEF FOR RSCH & ENGRG

ATTN: STRAT & SPACE SYS (OS)

ATTN: STRAT & THTR NUC FOR J THOMPSON

ATTN: STRAT & THEATER NUC FORCES

DEPARTMENT OF THE ARMY

DEP CH OF STAFF FOR OPS & PLANS

ATTN: DAMO-NCZ

HARRY DIAMOND LABORATORIES

ATTN: SLCHD-NW-RH

U S ARMY MATERIAL COMMAND

ATTN: AMCCN

U S ARMY MATERIAL TECHNOLOGY LABORATORY

ATTN: DRXMR-HH

U S ARMY STRATEGIC DEFENSE CMD

ATTN: DACS-BM/TECH DIV

U S ARMY STRATEGIC DEFENSE COMMAND

ATTN: ATC-D WATTS

ATTN: ATC-R ANDREWS

DEPARTMENT OF THE NAVY

NAVAL RESEARCH LABORATORY

ATTN: CODE 2627 TECH LIB

ATTN: CODE 4040 D BOOK

NAVAL SEA SYSTEMS COMMAND

ATTN: SEA-0351

NAVAL SURFACE WEAPONS CENTER

ATTN: CODE K82

ATTN: CODE R44 H GLAZ

OFC OF THE DEPUTY CHIEF OF NAVAL OPS

ATTN: NOP 654 STRAT EVAL & ANAL BR

STRATEGIC SYSTEMS PROGRAMS(PM-1)

ATTN: SP-272

DEPARTMENT OF THE AIR FORCE

AIR FORCE SYSTEMS COMMAND

ATTN: DLW

AIR FORCE WEAPONS LABORATORY, AFSC

ATTN: NTED J RENICK

ATTN: NTED LT KITCH

ATTN: NTED R HENNY

ATTN: NTEDA

ATTN: NTES

ATTN: SUL

AIR FORCE WRIGHT AERONAUTICAL LAB

ATTN: FIBC

ATTN: FIMG

AIR UNIVERSITY LIBRARY

ATTN: AUL-LSE

DEPARTMENT OF THE AIR FORCE (CONTINUED)

AIR FORCE WRIGHT AERONAUTICAL LAB
ATTN: AFWAL/MLP
ATTN: AFWAL/MLTM

BALLISTIC MISSILE OFFICE/DAA
ATTN: CAPT T KING MGEN
ATTN: CC/MAJ GEN CASEY
ATTN: ENSR

DEPUTY CHIEF OF STAFF/AF-RDQI
ATTN: AF/RDQI

DEPUTY CHIEF OF STAFF/AFRDS
ATTN: AFRDS SPACE SYS & C3 DIR

STRATEGIC AIR COMMAND/NRI-STINFO
ATTN: NRI/STINFO

STRATEGIC AIR COMMAND/XPQ
ATTN: XPQ

161 ARG ARIZONA ANG
ATTN: LTCOL SHERER

DEPARTMENT OF ENERGY

UNIVERSITY OF CALIFORNIA
LAWRENCE LIVERMORE NATIONAL LAB
ATTN: D BURTON
ATTN: L-10 J CAROTHERS
ATTN: L-122 G GOUDREAU
ATTN: L-122 S SACKETT
ATTN: L-203 T BUTKOVICH
ATTN: L-22 D CLARK
ATTN: L-8 P CHRZANOWSKI
ATTN: L-84 H KRUGER

LOS ALAMOS NATIONAL LABORATORY
ATTN: A112 MS R SELDEN
ATTN: M T SANDFORD
ATTN: R WHITAKER

SANDIA NATIONAL LABORATORIES
ATTN: D J RIGALI 1650
ATTN: ORG 7112 A CHABAI
ATTN: R G CLEM 1600

OTHER GOVERNMENT

CENTRAL INTELLIGENCE AGENCY
ATTN: OSWR/NED

DEPARTMENT OF THE INTERIOR
ATTN: D RODDY

DEPARTMENT OF DEFENSE CONTRACTORS

ACUREX CORP
ATTN: C WOLF

AEROSPACE CORP
ATTN: H MIRELS

APPLIED RESEARCH ASSOCIATES, INC
ATTN: N HIGGINS

APPLIED RESEARCH ASSOCIATES, INC
ATTN: S BLOUIN

APPLIED RESEARCH ASSOCIATES, INC
ATTN: D PIEPENBURG

BELL AEROSPACE TEXTRON
ATTN: C TILYOU

CALIFORNIA RESEARCH & TECHNOLOGY, INC
ATTN: K KREYENHAGEN
ATTN: M ROSENBLATT

CALIFORNIA RESEARCH & TECHNOLOGY, INC
ATTN: F SAUER

G. B. LABORATORY, INC
2 CYS ATTN: G H BURGHART

H-TECH LABS, INC
ATTN: B HARTENBAUM

INFORMATION SCIENCE, INC
ATTN: W DUDZIAK

KAMAN SCIENCES CORP
ATTN: L MENTE
ATTN: R RUETENIK
ATTN: W LEE

KAMAN TEMPO
ATTN: DASIAC

KAMAN TEMPO
ATTN: DASIAC

MAXWELL LABORATORIES, INC
ATTN: J MURPHY

MERRITT CASES, INC
ATTN: J MERRITT

NEW MEXICO ENGINEERING RESEARCH INSTITUTE
ATTN: G LEIGH

PACIFIC-SIERRA RESEARCH CORP
ATTN: H BRODE, CHAIRMAN SAGE

R & D ASSOCIATES
ATTN: A KUHL
ATTN: C K B LEE
ATTN: J LEWIS
ATTN: P RAUSCH

DEPT OF DEFENSE CONTRACTORS (CONTINUED)

R & D ASSOCIATES

ATTN: P MOSTELLER

S-CUBED

ATTN: A WILSON

S-CUBED

ATTN: C NEEDHAM

SCIENCE APPLICATIONS INTL CORP

ATTN: H WILSON

SCIENCE APPLICATIONS INTL CORP

ATTN: J COCKAYNE

ATTN: W LAYSON

SCIENCE APPLICATIONS INTL CORP

ATTN: A MARTELLUCCI

SCIENCE APPLICATIONS INTL CORP

ATTN: G BINNINGER

TRW ELECTRONICS & DEFENSE SECTOR

ATTN: G HULCHER

ATTN: P DAI

WEIDLINGER ASSOC, CONSULTING ENGRG

ATTN: P WEIDLINGER

END

12-86

DTIC